Dust devils as observed by Mars Pathfinder

Francesca Ferri,[1,2] Peter H. Smith,[3] Mark Lemmon,[4] and Nilton O. Rennó[5]

[1] Dust devils are localized meteorological phenomena frequently observed in terrestrial dry lands and desert landscapes as well as on Mars. They are low-pressure, warm core vortices that form at the bottom of convective plumes and loft dust from the surface. They move with the speed of the ambient wind and are tilted by wind shears. The Mars Pathfinder detected dust devils as dust plumes in the Imager for Mars Pathfinder images and as low-pressure convective vortices in the meteorological Mars Pathfinder Atmospheric Structure Investigation/Meteorology (ASI/MET) experiment data. The Pathfinder data have been analyzed in terms of dust devil size, spatial distribution, and frequency of occurrence. The results show that the Pathfinder imaging and MET observations are consistent with each other and with the observations made by the Viking 1 Orbiter and Mars Global Surveyor. The dust devil's ability to loft dust into the atmosphere has been investigated and a thermodynamic theory for dust devils has been used to calculate their physical parameters relevant to dust transport. The dust devils observed in an active day provide a pumping rate larger than the dust-settling rate derived from the optical obscuration of the Pathfinder rover solar panels. Therefore dust devils are a major factor in transporting dust from the surface to the atmosphere at the Pathfinder site.   *INDEX TERMS:* 6225 Planetology: Solar System Objects: Mars; 5409 Planetology: Solid Surface Planets: Atmospheres—structure and dynamics; 3322 Meteorology and Atmospheric Dynamics: Land/atmosphere interactions; 5445 Planetology: Solid Surface Planets: Meteorology (3346); *KEYWORDS:* dust devils, Mars, Pathfinder

Citation: Ferri, F., P. H. Smith, M. Lemmon, and N. O. Rennó, Dust devils as observed by Mars Pathfinder, *J. Geophys. Res.*, *108*(E12), 5133, doi:10.1029/2000JE001421, 2003.

1. Introduction

[2] When the midday Sun heats the ground, warm air immediately above the surface raises generating convective plumes. As pockets of warm air rise, they frequently interact with the ambient wind field and causes air moving toward the center of the updraft to spin while attempting to conserve angular momentum. Surface friction reduces the angular momentum of the spinning air parcels and perturbs the balance between centrifugal and pressure gradient forces. The decrease in the centrifugal forces makes the near surface warm air to nconverge toward the vortex center. The radial inflow into the rising plume, in turn, increases the concentration of the ambient vorticity. If dust is entrained in the rising vortex, it becomes a dust devil. The conditions for the generation of these convective vortices are the combined coexistence of deep convective plumes and ambient vorticity.

[3] The existence and intensity of a dust devil depends on the depth of the convective plume and the presence of wind shears. Intense free convection occurs under conditions of deep convective layer, super-adiabatic temperature lapse rate, and strongly heated surface (large surface heat flux). The Viking and Pathfinder landers confirmed that these conditions are met near local midday in the summer hemisphere of Mars, where dust devils are frequently observed between 9 am to 3 pm local time. They last as long as the convective plume is active and vorticity is present. When a dust devil moves across a cold terrain, the convective plume is cut-off by the decrease in surface heat flux and the dust column disappears.

[4] Dust devils have been observed on Mars by the Vikings orbiters and landers [*Ryan and Lucich*, 1980; *Thomas and Gierasch*, 1985], by the Mars Pathfinder [*Schofield et al.*, 1997; *Metzger et al.*, 1999] and by the Mars Global Surveyor (MGS) camera [*Edgett and Malin*, 2000]. MGS images show an extensive network of dust devil tracks globally distributed around the planet and changing seasonally.

[5] Dusty conditions seem to be normal in the Martian atmosphere as shown by observations from ground and space. Even before their detection, Martian dust devils have been hypothesized to be important in the initiation of large dust storms [*Neubauer*, 1967; *Gierasch and Goody*, 1973]

[1]Center of Studies and Activities for Space (CISAS), "G. Colombo," University of Padova, Padova, Italy.
[2]Also at Planetary and Space Sciences Research Institute (PSSRI), Open University, Milton Keynes, UK.
[3]Lunar and Planetary Laboratory, University of Arizona, Tucson, Arizona, USA.
[4]Texas A and M University, College Station, Texas, USA.
[5]Department of Atmospheric, Oceanic and Space Sciences, University of Michigan, Ann Arbor, Michigan, USA.
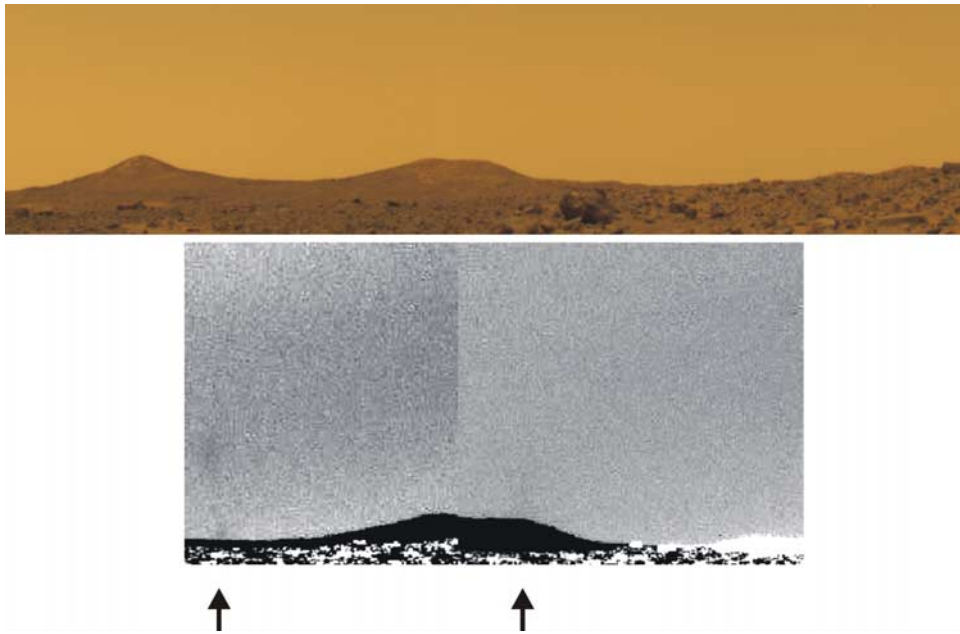
Figure 1. Twin Peaks and dust devils over the North Peak. Top: true color image of Mars based upon three filters (670, 530 and 440 nm), showing the panorama including the Twin Peaks as seen from the Pathfinder. The image has been derived from the frames taken near local noon on sol 10. There exist two dust devils ("167" and "161") hidden in the haze, near the North Twin Peak. They are revealed in the blue filter frames by flat field correction and contrast enhancement. Bottom: two dust plumes are barely visible in two panorama frames in blue filter taken ∼6 min apart, looking at the North Twin Peak (the white spots on the horizon at the right and on the land are just ghosts of the Martian surface present in the frame used as flat field).

and in the maintenance of the general atmospheric dust content [*Ryan and Lucich*, 1980]. In the absence of other dust entrainment mechanisms, the Martian dust-settling rate is rapid enough to clear the atmosphere over a period of a few weeks after a global dust storm [*Pollack et al.*, 1979]. Some process replenishes atmospheric dust to maintain the constant optical depth observed by past Mars Landers. Strong local vortices (dust devils) are more efficient in entraining dust from the surface into the atmosphere than horizontal winds. Therefore dust devils may be the primary dust entrainment mechanism on Mars.

[6] We have searched all Pathfinder's horizon images for faint dust devils, and Mars Pathfinder Atmospheric Structure Investigation/Meteorology (ASI/MET) observations to detect signatures of the passage of small-scale vortices over the Pathfinder meteorological sensors. The location and size of the dust devils observed in images have been estimated using a model based only on the assumption that they move with the speed of a constant ambient wind. A scaling theory for dust devils [*Rennó et al.*, 1998, 2000] is used to calculate the values of the physical parameters of Martian dust devils and to estimate their potential to pump dust into the atmosphere.

2. Data Analysis

[7] In the Pathfinder data set, dust devils have been detected as dust plumes in the images and as convective vortices in the ASI/MET temperature, pressure and wind measurements. Fourteen dust plumes were found in Imager

for Mars Pathfinder (IMP) images containing the horizon. A possible detection, not confirmed by other data, has been recorded in the atmospheric opacity data. The pressure sensor has recorded the signatures of the passage of 79 vortices. None of these events have been verified with images because of the lack of simultaneous measurements in both instruments.

3. Dust Plumes in the Imager for Mars Pathfinder Images

[8] The Martian atmosphere is dusty, and the sky at the horizon has essentially the same color as the dust devils with a contrast of typically 1–3%. Dust devils, illuminated by the Sun, appear as dark shadow plumes. The presence of the dust plumes in the images of the Imager for Mars Pathfinder (IMP) has been revealed through contrast manipulation. Since the Martian aerosols have a low reflectance in blue wavelengths, it is easier to detect dust devils in images taken with the blue filter (440 nm).

[9] A true color image of the Martian sky at the horizon, based upon the superposition of three filters (red, green, and blue) is shown at the top of Figure 1. The image, showing the panorama including the Twin Peaks as seen from the Pathfinder, has been derived from frames taken near the local noon on sol 10. There are two dust devils hidden in this image. They are revealed through contrast enhancement of the frames in the blue filter.

[10] Previous work, using spectral differencing techniques revealed five localized dust plumes in IMP images

Table 1. Dust Devils Found in IMP Images[a]

Dust Devil Number	Date	Time, h	Azimuth, deg	Estimated Distance, km	Estimated Size, m
002	Sol 2	15:06:03	91.0	6.98	–
149	Sol 10	11:16:59	334.2	5.51	–
Couch	Sol 10	11:34:12	305.7	17.18	245 230[b]
161	Sol 10	11:40:30	287.3	13.86	92 145[b]
165	Sol 10	11:52:12	262.3	7.93	126
167	Sol 10	11:58:12	250.2	1.67	15 11[b]
STP	Sol 11	12:16:08	230.1	4.52	76 114[b] 58[c]
Vague	Sol 11	12:22:01	222.8	2.68	–
177	Sol 11	12:33:47	196.5	1.02	–
Small	Sol 11	12:39:40	187.6	10.82	103 135[b]
MMfar	Sol 11	12:45:40	177.3	15.42	455 221[b]
MMnear	Sol 11	12:45:40	182.1	6.55	242 196[b]
183	Sol 11	12:51:32	166.8	24.03	573
387	Sol 11	12:34:55	203.3	5.95	84 132[b]

[a]IMP, Imager for Mars Pathfinder.
[b]Estimated in images taken with green filter.
[c]Estimated in images taken with red filter.

acquired at midday [*Metzger et al.*, 1999]. Our survey, based on contrast manipulation of frames with different filters, resulted in the detection of new dust devils and in the determination of the position and size of the dust plumes. We also monitored the motion of these dust plumes as multifilter images of the same scene were acquired. All IMP images containing the horizon were searched for dust features. The analysis consists of varying the contrast range of the images divided by a flat field in order to distinguish localized dust plumes from the general haze. The sky flat field was selected from a frame of the same sol containing large portion of sky.

[11] Almost all frames containing features recognized as dust devils are from "Gallery Panorama" sequence from sols 10 and 11. The only exception is a dust devil detected on sol 2, before the IMP mast was deployed. For the Gallery Panorama sequence, the IMP camera stepped in a counter-clockwise direction sequentially imaging through the red (670 nm), green (530 nm) and blue (440 nm) filters [*Smith et al.*, 1997a]. During sol 10, the IMP imaged an area between azimuths 248° and 360° with the top of the frame at 13° in elevation, between ~11 am and 12 am (local time); on sol 11 the azimuth range was from 126° to 262° between 12 am and 1 pm. The only other frame containing a dust plume was recorded on sol 2 at 89.8° azimuth at 3 pm. Fourteen contrast features in the IMP blue filter images have been recognized as dust devils (see Table 1). Nine of them have also been observed in the green filter and three also in the red filter. Since the time interval for changing filters and acquiring new images is ~20 s, the change in the azimuth position of the dust plumes in images with different filters indicates their angular velocity. Figures 1, 2, 3 and 6 show some of the dust plumes detected by this survey. Figure 2 shows the same dust devil ('STP') as observed at the three different filters near local noon on sol 11 near South Twin Peak (~233° in azimuth). The dust devil moves from 1°, from 231° to 230°, in a time span of 36 s.

[12] The IMP images containing dust devils and the frames used as flat field are listed in Table 2 as reference. Another potential detection of a dust devil passage by IMP is suggested by the sudden increase of the atmospheric opacity on sol 14. The atmospheric extinction caused by dust has been monitored throughout the mission by imaging the sun at different filters [*Smith et al.*, 1997b]. On sol 14 the opacity was mostly stable, except for a single event at 11:00 am when the opacity value was up to ~0.1 in all filters (see Figure 4); this transient event may be a dust devil [*Smith and Lemmon*, 1999]. There are no simultaneous
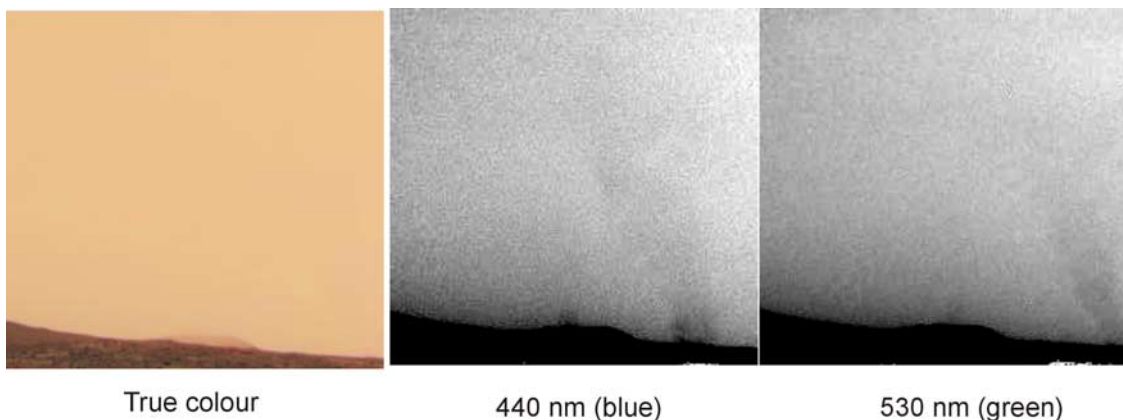

| True colour | 440 nm (blue) | 530 nm (green) |

Figure 2. Image taken on sol 11 at ~12:45 pm local time. The true color image on the left was derived from a combination of the three filters. At the horizon, it is possible to distinguish a misty mountain: Far knob (at ~30.6 km from the lander). Two dust plumes are hidden in the haze. Their presence is revealed by contrast enhancing of images taken with blue and green filters. The two dust plumes ("MM near" and "MM far") move from west to east. In the red filter (not shown) the central dust devil is visible, while only the upper part of the dust plume is seen on the image on the right, because the dust devil was still out of the field of view of the camera.
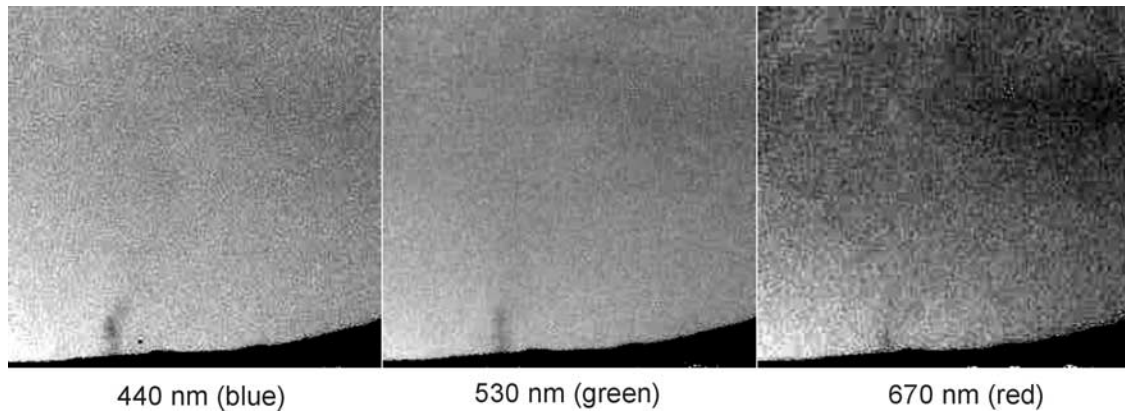
| 440 nm (blue) | 530 nm (green) | 670 nm (red) |

Figure 3. A dust plume as observed in images with the three different filters near the South Twin Peak at local noon on sol 11. The dust devil position has been determined in images with different filters. Images with the red filter (670 nm) (the one at the right side) shows a faint dust devil ("STP") that can be seen in subsequent images, with green filter (530 nm) at the center, and with blue filter (440 nm) on the left, the dust devil is moves from north to south while being imaged.

meteorological measurements to confirm whether or not a vortex passed over the lander at this same time.

4. Location and Size of the Dust Plumes

[13] The location and size of observed dust plumes have been estimated from their azimuth position and angular width on the IMP frames, on the basis of geometrical considerations, and the assumption that dust devils move with the ambient wind. The ambient wind is assumed to maintain a constant velocity and direction each day between 9 am and 3 pm.

4.1. Azimuth Position and Angular Width of the Dust Plumes

[14] The azimuth position of dust plumes and their angular size have been empirically determined by measuring the obscuration feature that a dust devil generates against the

Table 2. IMP Images Containing Dust Devils

| Dust Devil Name	Sol	Local Standard Time, h	Image File Name	Filter
002	2	15.101	i1246853726l.img_0030020002	blue
149	10	11.283	i1247556039r.img_0164020149	blue
Couch	10	11.576	i1247557124r.img_0164020157	blue
		11.571	i1247557104r.img_0164020087	green
161	10	11.675	i1247557488r.img_0164020161	blue
		11.669	i1247557468r.img_0164020091	green
165	10	11.870	i1247558212r.img_0164020165	blue
		11.865	i1247558193r.img_0164020095	green
167	10	11.970	i1247558577r.img_0164020167	blue
		11.964	i1247558557r.img_0164020097	green
STP	11	12.269	i1247648441r.img_0165020171	blue
		12.264	i1247648422r.img_0165020101	green
		12.259	i1247648405r.img_0165020031	red
Vague	11	12.367	i1247648803r.img_0165020173	blue
177	11	12.563	i1247649531r.img_0165020177	blue
Small	11	12.661	i1247649893r.img_0165020179	blue
		12.657	i1247649878r.img_0165020109	green
		12.654	i1247649861r.img_0165020039	red
MM	11	12.761	i1247650261r.img_0165020181	blue
		12.755	i1247650241r.img_0165020111	green
		12.751	i1247650224r.img_0165020041	red
183	11	12.859	i1247650625r.img_0165020183	blue
		12.855	i1247650606r.img_0165020113	green
387	11	12.582	i1247649609r.img_0165020387	blue
Frames used as flat fields				
FF	2	13.512	i1246854235l.img_0030020014	blue
FF	10	11.772	i1247557849r.img_0164020163	blue
FF	10	11.768	i1247557830r.img_0164020093	green
FF	11	12.465	i1247649166r.img_0165020175	blue
FF	11	12.483	i1247649240r.img_0165020385	blue
FF	11	12.657	i1247649878r.img_0165020109	green
FF	11	12.259	i1247648405r.img_0165020031	red
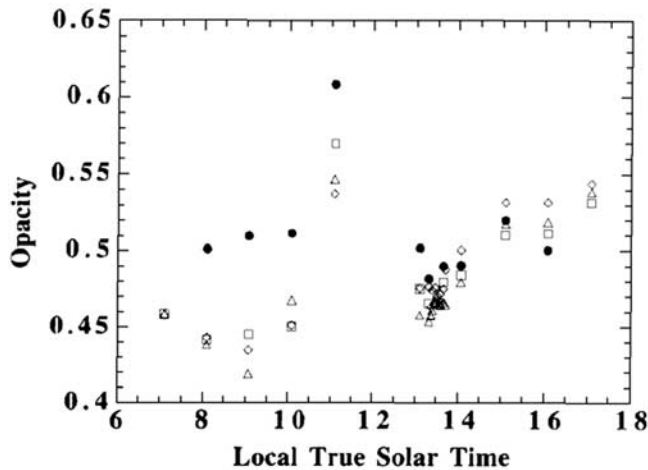
Figure 4. Atmospheric opacity versus local time derived from images with filters of 450 nm (circle), 670 nm (squares), 883 nm (diamonds), and 989 nm (triangles) on sol 14 [*Smith and Lemmon*, 1999]. The high opacity recorded in all filters at 11:00 must have been a transient event like a dust devil or dust plume.

sky. In order to reduce noise, the pixel values from the columns in one JPEG compression block (8×8 pixels) have been averaged (see Figure 5). The azimuth position has been assumed to correspond to the minimum intensity, while the angular width has been measured at the half intensity values. Estimating the azimuth motion of the same dust plume in frames taken with different filters, the angular velocity of the dust devil has been calculated. All dust devils observed on sol 10 move clockwise, while the ones on sol 11 move counterclockwise. Some of the dust plumes are tilted, probably forced by wind shear; the ones from sol 10 are tilted toward the right, while those from sol 11 toward the left. The dust devil observed on sol 2 ($\sim 91°$ azimuth) is tilted toward the right (see Figure 6). If we assume that the dust devils move at the speed of the ambient wind, this suggests that the ambient wind is blowing from southwest and that wind shear tilts the tops forward (Figures 7 and 8).

[15] A simple geometrical model was developed to determine the actual distance and size of the dust devils, under the assumption that they move with the ambient wind. The ASI/MET data [*Schofield et al.*, 1997] suggests that during the time in which dust devils were observed (from 9 am to 3 pm) the wind was blowing from southwest. Considering the ASI/MET measurements of the wind direction [*Schofield et al.*, 1997] and the wind velocity observed by the Viking 1 [*Seiff and Kirk*, 1977], we assumed a uniform ambient wind of 10 m/s from 240° (azimuth). What we observe in the images is the apparent position of these dust plumes as projected on the horizon. A priori, we do not know their distance or true height above the ground (their bottoms could be hidden below the horizon). Moreover, we detect just the part of dust plume which is shadowed, and that depends on the relative orientation of the Sun and the axis of the dust column. Considering that the camera is mounted on a deployable boom at 1.5 m above the surface [*Smith et al.*, 1997a], the maximum detectable distance for a 1-km high plume, filling up at least a JPEG compression block (8x8 pixels) above the horizon, has been geometrically computed to be more than 50 km. However, the

dusty haze limits visibility and reduces contrast. The furthest geological feature detected on IMP images is Far Knob, which is located at 30.6 km from the lander; it looks like a misty mountain.

[16] Simple geometrical considerations (see Figure 6) determine the location of the observed dust plumes with respect to the lander. Since the dust devils are pushed by the wind, the time interval between consecutive frames in different filters multiplied by the wind speed gives the distance $D = \Delta t * v_{wind}$ that the dust devil has traveled. The distances from the Pathfinder lander to dust devils, at the different instants (as the same dust plume is imaged in different filters) are given by

$$d_1 = D \frac{\sin(\vartheta_2 - \alpha)}{\sin(\vartheta_2 - \vartheta_1)} \qquad (1)$$

$$d_2 = D \frac{\sin(\vartheta_1 - \alpha)}{\sin(\vartheta_2 - \vartheta_1)} \qquad (2)$$

where α is the assumed wind direction, θ_1 and θ_2 are respectively the azimuth positions of the dust devil in consecutive images with different filters, and D is the true distance traveled by the plume.

[17] There are three independent ways of estimating the true distance of dust devils from the lander:

[18] 1. First, the ambient wind velocity transporting the dust devil is assumed to be 10 m/s and 240° which leads to solution for (1) and (2). Among all dust devils found in IMP images, the closest one was at 1.5 km from the lander while the furthest was at 24 km.

[19] 2. The second method can be used with even a single sighting by assuming a typical diameter for dust devils and calculating their distance with the measured angular width. The two methods should be consistent. The derived sizes of observed dust plumes range from 15 to more than 550 m, but the peak of the distribution is between 100 and 200 m as shown in Figure 9. These results are consistent with the values estimated from images of shadows of dust plumes, taken by the Viking 1 orbiter [*Thomas and Gierasch*, 1985].

[20] 3. The third estimate of the size of Martian dust devils is based on the duration of their pressure drop while moving over the Pathfinder MET station (see next section). The size of the vortices detected by the ASI/MET package were determined by assuming that they were moving with an ambient wind of 10 m/s. The sizes obtained by this method are consistent with the values derived geometrically from images of the plumes.

4.2. Dust Devils as Detected by the Meteorological Experiment

[21] Several events in the meteorological data collected by the Viking 1 and 2 [*Ryan and Lucich*, 1980] and Pathfinder [*Schofield et al.*, 1997] landers have been interpreted as the passage of convective vortices. These events are characterized by short term variations in the measured surface pressure, wind direction and air temperature over periods of tens of seconds. The distinctive property of these events is a drop in the atmospheric pressure associated with a rotating wind vector. Specifically the Pathfinder Atmospheric Structure Instrument/Meteorological Package (ASI/MET) recorded
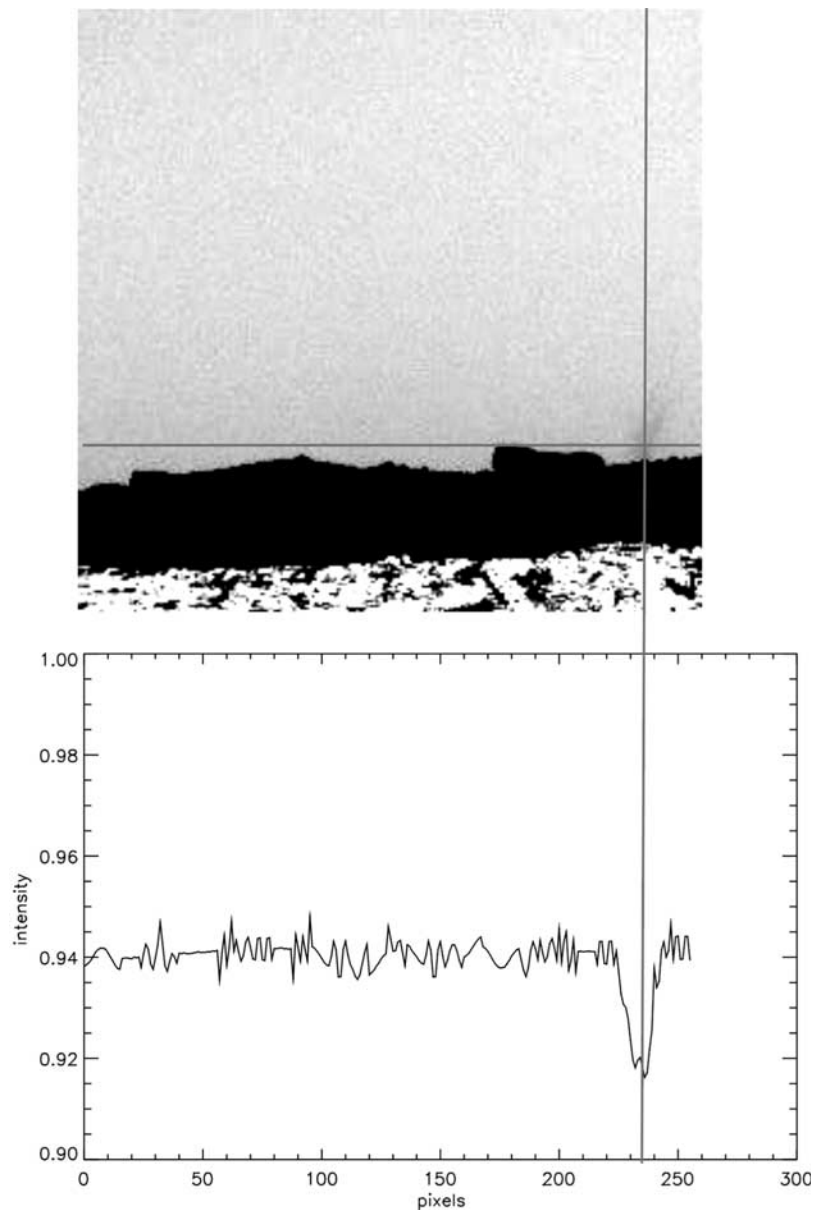
Figure 5. Determination of the azimuth position and angular width of dust devils from their obscuration features. In images taken on sol 10 a dust devil is visible on the right of the rock "Couch." Each point at the plot at the bottom shows the value of the intensity of one JPEG compression block (8 pixels wide). The presence of a dust devil is clearly detectable through the drop in light intensity. The azimuth position and width of the dust devil are determined by the location of the minimum value of the intensity and the width at half maximum.

the passage of 79 vortices during the 83 sol mission [*Murphy and Nelli*, 2002] when the atmospheric physical conditions were monitored continuously with a sampling rate adequate to detect dust devils, at the time period that they are expected to occur. In Table 3 are reported 19 of these events for which we have derive the duration of the pressure drop.

[22] Figure 9 shows the signature of the passage of a dust devil recorded by the ASI/MET sensors on sol 25. The data shows a rapid pressure drop accompanied by shifts in wind direction. The duration of the pressure minimum gives an indication of the dimension of the vortex core. The measured amplitude of the pressure drop during the nineteen events recognized to be vortices, or dust devils, is on average of 20 s.

Assuming that the vortices move with an ambient wind of 10 m/s, that corresponds to a core size of 200 m. This value is consistent with the geometrical calculation of dust devil sizes from dust plumes detected in IMP images. This method of measuring a vortex size gives a minimum, because it is not possible to know if their centers passed over the ASI/MET sensors.

5. Statistics

[23] The size and number of dust devils detected by the Pathfinder ASI/MET and imager (IMP), are used to statistically estimate the fractional area of the planet covered by
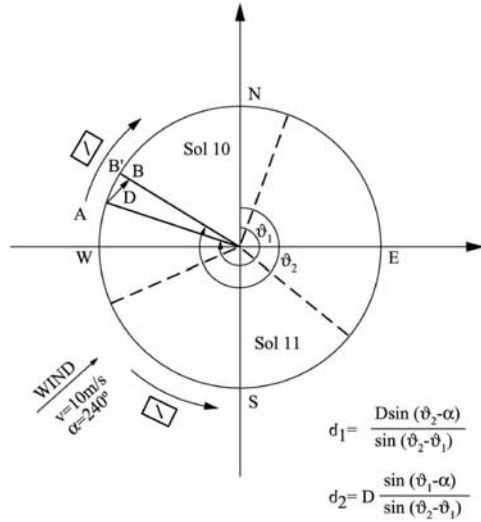
Figure 6. Our geometrical scheme to determine dust devils distance from the camera as they move with ambient wind blowing from 240°. The circle centered at the Pathfinder lander represents the distance to the dust plumes first seen in the Imager for Mars Pathfinder (IMP) frames. In reality, a dust devil could be located closer or farther away from the lander and therefore inside or outside the horizon circle. Assuming that dust devils move with the ambient wind (10 m/s, direction 240°), a dust devil, positioned in A, when imaged in subsequent frames, will be in B, having moved D meters in the wind direction. B' is the apparent position on the horizon. The dashed lines mark the sector areas observed during sols 10 and 11. The arrows outside the horizon circle represent the angular movement of dust devils observed on sols 10 and 11, while the box illustrates the vertical trend of the dust plumes sloping with the wind shear.

dust devils. Referring to the meteorological data, the average dust devil has a diameter of $\sim$200 m, while the IMP data showed 6 dust devils in panoramic images of an active day. The images cover an area of $\sim$9 $\times$ 10^8 m^2 (a region of $\sim$30 km of radius over a sector of 120°). Considering that the panoramic images were taken during the 6 hours period of time in which dust devils are expected to occur (from 9 am to 3 pm), this results in $\sim$2 $\times$ 10^{-4} fraction of the surface is covered by dust devils during their active period (9 am to 3 pm). Thus statistically $\sim$0.5 $\times$ 10^{-4} of the Martian surface is covered by dust devils.

6. A Thermodynamic Model of a Dust Devil

[24] A thermodynamic theory for dust devils [*Rennó et al.*, 1998, 2000] is used to compute their intensities and the values of their physical parameters relevant to the transport of dust. The theory suggests that the presence of both convection and mechanisms for the generation of vorticity is essential for the genesis of dust devils. Since the flow around a dust devil is, to a first approximation, in cyclostrophic balance, the bulk pressure drop between the ambient and its center determines its tangential wind speed. The bulk pressure drop, in turn, depends solely on the thermodynamics of the dust devil convective heat engine. Thus to a

first approximation, the wind speed around a dust devil is determined uniquely by the thermodynamics of its convective heat engine. The tangential wind speed around a dust devil is given by

$$ v_a \sim \sqrt{\frac{R T_S \Delta p}{p_S}} \qquad (3) $$

where R is the atmospheric specific gas constant, T_s and p_s are the ambient surface air temperature and pressure, and Δp is the radial pressure drop across the vortex [*Rennó et al.*, 1998].

[25] The pressure drop across a dust devil [*Rennó et al.*, 1998, see equation (16)] is given by

$$ \Delta p \equiv p_\infty - p_0 \approx p_\infty \left(1 - \exp\left[\left(\frac{\gamma\eta}{\gamma\eta - 1} \right)\left(\frac{c_p}{R} \right)\left(\frac{T_0 - T_\infty}{T_\infty} \right) \right] \right) \qquad (4) $$

where p_0 and T_0 are the temperature and pressure at the vortex center, $p_\infty = p_s$ and $T_\infty = T_s$ are the temperature and pressure at large radial distance from the vortex center, γ is the fraction of the mechanical energy consumed by friction near the surface, η is the thermodynamic efficiency, and c_p is the atmospheric heat capacity at constant pressure per unit mass. The fraction of the total dissipation of mechanical energy has been estimated to be $\gamma \sim 1$ and the thermodynamic efficiency $\eta \sim 0.15$ both on Earth and on Mars [*Rennó et al.*, 1998, 2000].

[26] The magnitude of the vertical wind speed within a dust devil can be computed by equation (42) of *Rennó and Ingersol* [1996], that is

$$ w \approx \sqrt{\frac{c_p}{8\varepsilon\sigma_R T_c^3}\frac{\eta F_{in}}{\mu}} \qquad (5) $$

where $\varepsilon \sim 0.5$ is the thermal emissivity of the convective layer air, $\sigma_R \sim 5.67{*}10^{-8}$ Wm^{-2}K^{-4} is the Stefan-Boltzmann constant, T_c is the mean temperature of the convective layer, F_{in} is the input heat flux into the convective heat engine (the surface sensible heat flux), and μ is a dimensionless coefficient of turbulent dissipation of mechanical energy [*Rennó and Ingersol*, 1996]. To estimate μ, both the length of the convective path (that is of the convective circulation) and the length and velocity scale of the most energetic eddies must be known [see *Rennó and Ingersol*, 1996]. Since in homogeneous and isotropic turbulence the most energetic eddies are the largest, we arbitrarily assume that the most energetic eddies have the length and velocity scale of the convective drafts. Assuming that the length of the convective path is $\sim$8 times the thickness of the convective layer we estimate that $\mu \sim 50$ [*Rennó and Ingersol*, 1996; *Rennó et al.*, 2000]. Using the above equations and the typical values of the meteorological parameters observed by the Pathfinder ASI/MET (surface average temperature $T_s = 250$ K, pressure $p_s = 7$ hPa, $T_c = 200$K), we calculate the temperature perturbation pressure drop, tangential, and vertical velocities in Martian dust devils.
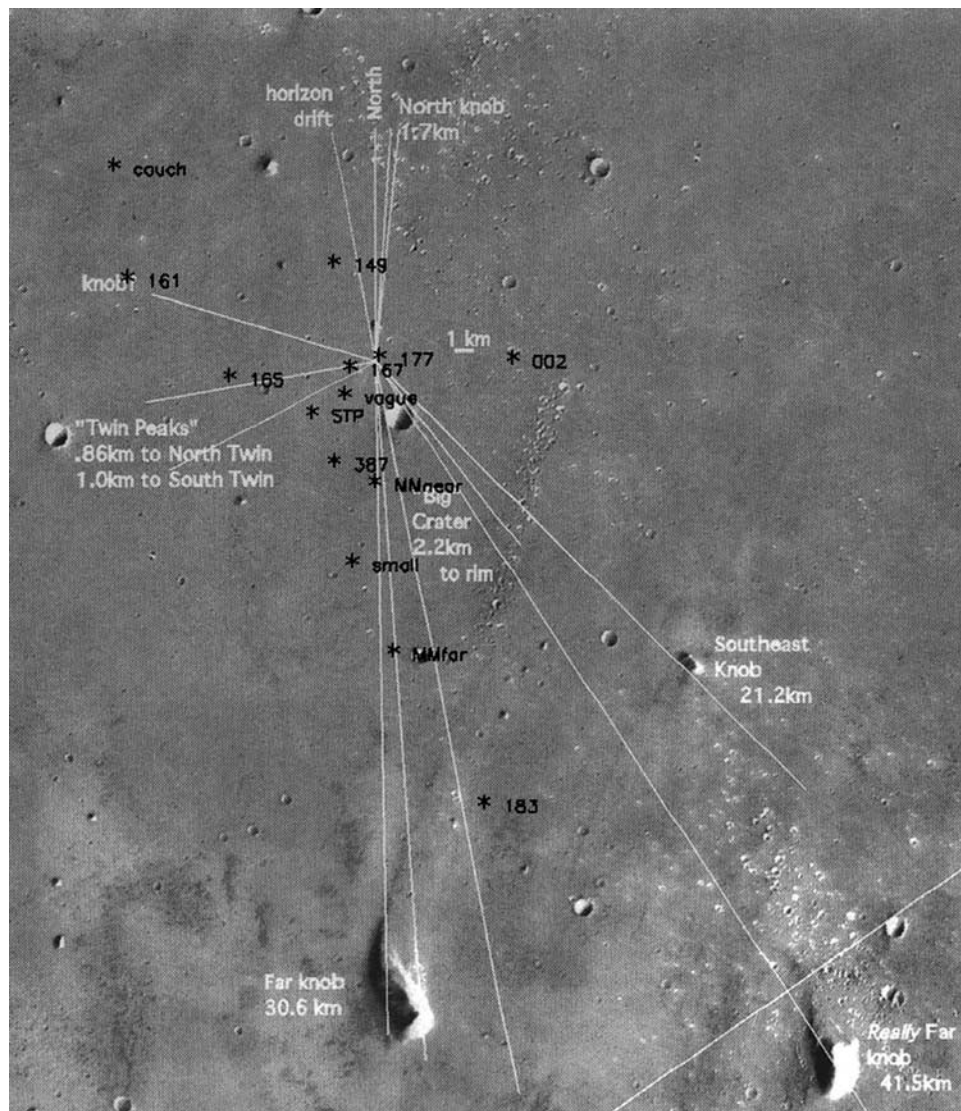
Figure 7. The Mars Pathfinder landing site and the spatial distribution of the observed dust devils on the Martian surface. Some surface features and their relative distance from the lander are shown, while the dust devil positions have been marked with asterisks. The positions at which the dust devils were located were estimated through geometrical considerations, assuming a uniform ambient wind of 10 m/s from 240°; the distance of those dust devils observed only in the blue filter were estimated assuming that they were 200 m wide.

[27] The work performed by a dust devil convective heat engine is proportional to the radial pressure drop across its center. Therefore the pressure drop provides a good estimation for their intensity. Since ASI/MET measured this pressure drop across some weak vortices ($\leq$ 0.03 hPa), it is possible to derive the value of the temperature at their center, or equivalently the value of the difference of temperature between the air inside and outside the vortex as $\Delta T \leq 1.2$ K. This value is consistent with Pathfinder's observations of the temperature perturbations in these weak, dust free vortices. It follows from equation (3) and (4) that the tangential velocity around a thermodynamically efficient dust devil (with convection extending though at least one temperature scale height) is ~20 m/s. These are the typical dusty dust devils. In addition, the magnitude of the vertical component of the wind velocity within these dust devils, computed by equation (5), is w = 20 m/s.

7. Role of Dust Devils in Mars' Atmosphere

[28] The role of dust devils is investigated on the basis of the Pathfinder data to determine their importance in entraining dust in the atmosphere. Dust devils have been hypothesized to be important in the initiation of large dust storms and as a source for the general atmospheric dust content [*Neubauer*, 1967; *Gierasch and Goody*, 1973; *Ryan and Lucich*, 1980; *Smith and Lemmon*, 1999]. Because of their large vertical velocities and turbulent flow near the ground, dust devils are thought to be much more efficient in pumping dust into the atmosphere than horizontal winds.
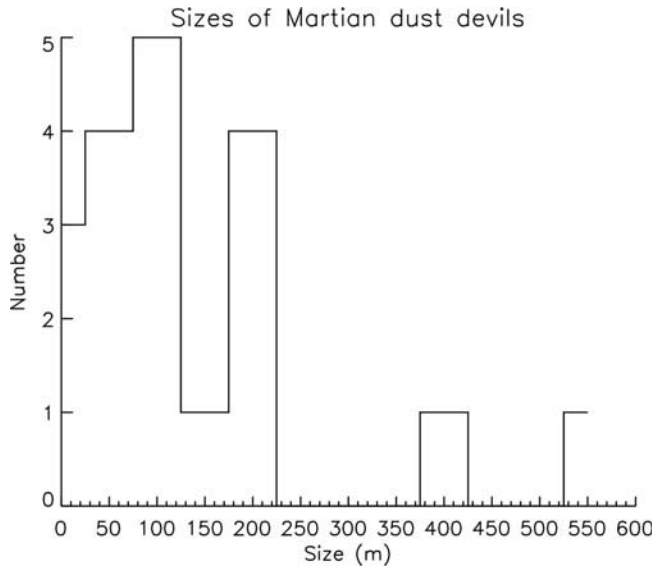
Figure 8. Histogram of dust devil diameters as observed in the Pathfinder imager frames. The diameters of dust devils observed in two consecutive IMP frames were estimated geometrically, knowing their angular size and distance from the lander.

Table 3. Mars Pathfinder ASI/MET Observations[a]

Sol	Local Time	Pressure Drop, 10^{-1} Pa	Sample Interval, s	Duration, s
25	13:10	12	4	15
25	13:53	28	4	27
34	09:52	17	1	22
34	11:32	46	1	18
34	11:38	22	1	39
38	12:32	23	4	51
39	11:31	12	4	51
39	13:47	45	4	33
49	11:02	15	4	–
52	12:03	12	4	42
55	14:19	18	4	31
60	10:09	17	4	17
62	12:34	14	4	25
62	13:31	13	4	16
62	14:06	30	4	40
68	11:42	24	4	14
68	13:29	22	4	23
69	12:54	11	2	17
70	14:25	11	2	25

[a]"Dust devil" passages as indicated by measured pressure drops.

[29] In the case of the Pathfinder, an increase in the atmospheric opacity throughout the mission [*Smith and Lemmon*, 1999] occurred even as dust settling was observed onto the solar panels [*Rover Team*, 1997; *Landis and Jenkins*, 2000] and the magnetic arrays [*Hviid et al.*, 1997; *Madsen et al.*, 1999]. The variation in the atmospheric dust content from morning to night appears related to the occurrence of dust devils at midday, therefore dust devils have been suggested to be the primary suppliers of dust to the atmosphere of the Ares Vallis region [*Smith and Lemmon*, 1999]. The computed wind velocities (see previous section) of thermodynamically efficient Martian dust devils are strong enough to initiate the process of saltation of loose surface material [*Pollack et al.*, 1976; *Greeley et al.*, 1980] and consequently to propel sand particles via a skipping motion and loft dust into the atmosphere.

[30] The atmospheric dust loading due to dust devils is calculated on the basis of the results of our analysis, and IMP atmospheric opacity data. The dust devils observed in the images of the Mars Pathfinder panoramic camera have ~700 times the dust content of the local background atmosphere [*Metzger et al.*, 1999]. The dust content across a typical Martian dust devil is estimated to be Ld = 7×10^{-4} kg/m³, where L is the path length through the dust devil and d is its dust load [*Metzger et al.*, 1999]. It follows from this that a 200 m dust devil has a load of 3.5×10^{-6} kg/m³. Assuming a typical vertical velocity of 20 m/s, we find that dust flux in these dust devils is 7×10^{-5} kg/m²s.
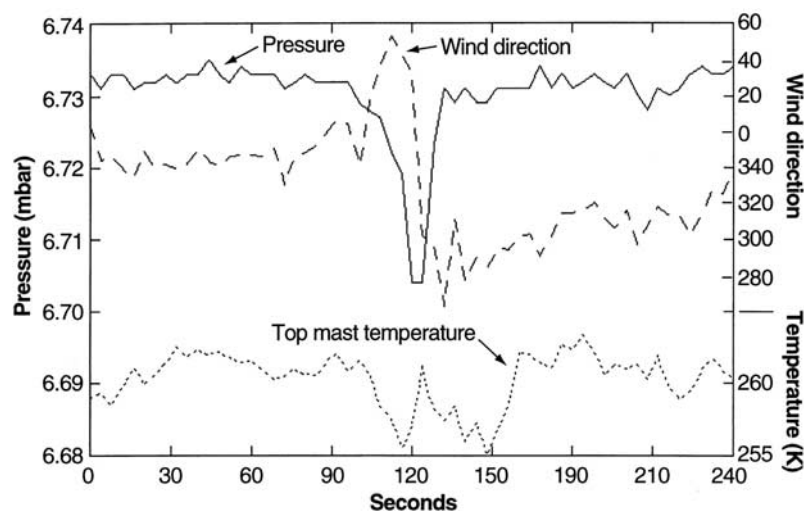

Figure 9. Dust devil signature in the meteorological data of Pathfinder Atmospheric Structure Investigation/Meteorology experiment [*Schofield et al.*, 1997]. The plot shows the pressure, wind direction and temperature variations associated with a small dust devil, passing over the lander on sol 25 at 11:30 am, LST. The measurements were taken at 4-s intervals. The pressure drop is accompanied by a shift in wind direction.

Since the fractional area covered by dust devils in an active day is 2×10^{-4} (see section 4), the dust flux due to dust devils is $\sim 3.6 \times 10^{-9}$ kg/m^{2}s at this particular day. This flux is an order of magnitude larger than the observed deposition rate of 3×10^{-10} kg/m^{2}sl [*Rover Team*, 1997; *Landis and Jenkins*, 2000]. Given the uncertainties of our calculations and data analysis, this result confirms that dust devils contribute significantly to the maintenance of dust in Mars' atmosphere, perhaps even being the primary suppliers of dust into the atmosphere of the Ares Vallis.

8. Conclusions

[31] Mars Pathfinder has detected dust devils as dust plumes in IMP frames and as convective vortices in ASI/MET measurements. A reanalysis of the Pathfinder data resulted in the detection of new features interpreted as dust devils. More than fourteen dust plumes (including five previously detected by *Metzger et al.* [1999]) have been detected in the IMP frames containing the horizon. Seventy-nine events in the meteorological records of the ASI/MET sensors have been interpreted as the passage of vortices that likely could contain dust.

[32] Their angular position and sizes within the frames have been measured. The angular velocity of the dust plumes imaged in different filters has been estimated. Starting with the assumption that dust devils move with a uniform ambient wind of 10 m/s, the location and actual size of the observed dust devils have been geometrically determined. The distance of the dust devils observed from the Pathfinder lander range from 1.5 km up to 24 km, while their size distribution is peaked at 100–200 m.

[33] The role of the dust devils in supplying dust to the Martian atmosphere has been investigated on the basis of the Pathfinder ASI/MET and IMP data. A simple physical model of the general characteristics of the Martian dust devils has been derived from a scaling theory developed to explain dust devils [*Rennó et al.*, 1998, 2000]. Through the use of this simple thermodynamic model of dust devils and the physical conditions monitored by ASI/MET, the intensity and physical parameters of Martian dust devils were estimated. The computed tangential velocities are strong enough to initiate saltation [*Pollack et al.*, 1977; *Greeley et al.*, 1980] and consequently to entrain dust into the Martian atmosphere. These results, while slightly different from the ones inferred by *Metzger et al.* [1999], are in very good agreement with the results of previous observations by the Viking orbiter [*Thomas and Gierasch*, 1985] and more recent observations by the Mars Global surveyor [*Edgett and Malin*, 2000].

[34] *Metzger et al.* [1999] calculated the dust loading within a Martian dust devil using a Montecarlo scattering model and the atmospheric opacity observations of the Pathfinder camera. Combining this value with statistical analysis of dust devil detections by the Pathfinder, the dust transport into the atmosphere has been estimated. The estimated value is comparable to the observed dust deposition rate on the rover solar panels [*Rover Team*, 1997; *Landis and Jenkins*, 2000] and the magnetic arrays [*Hviid et al.*, 1997; *Madsen et al.*, 1999]. This confirms that dust devils are a major source for entraining dust into the Martian atmosphere with pumping rate comparable to the dust settling rate as derived from the dust obscuration of the rover solar panels [*Rover Team*, 1997; *Landis and Jenkins*, 2000].

References

Edgett, K. S., and M. C. Malin, Martian dust raising and surface albedo controls: Thin, dark (and sometimes bright) streaks and dust devils in MGS MOC high resolution images, *Lunar Planet. Sci. Conf.*, *XXXI*, 1073, 2000.

Gierasch, P. J., and R. M. Goody, A model of a martian great dust storm, *J. Atmos. Sci.*, *30*, 169–179, 1973.

Greeley, R., R. Leach, B. White, J. Inversen, and J. Pollack, Threshold wind speeds for sand on Mars: Wind tunnel simulations, *Geophys. Res. Lett.*, *7*, 121–124, 1980.

Hviid, S. F., et al., Magnetic properties experiment on the Mars Pathfinder, *Science*, *278*, 1768–1770, 1997.

Landis, G. A., and P. P. Jenkins, Measurement of the settling rate of atmospgheric dust on Mars by the MAE instrument on Mars Pathfinder, *J. Geophys. Res.*, *105*, 1855–1857, 2000.

Madsen, M. B., S. F. Hviid, H. P. Gunnalaugsson, J. M. Knudsen, W. Goetz, C. T. Pedersen, A. R. Dinesen, C. T. Mogensen, M. Olsen, and R. B. Hargraves, The magnetic properties experiments on Mars Pathfinder, *J. Geophys. Res.*, *104*, 8761–8780, 1999.

Metzger, S. M., J. R. Johnson, J. R. Carr, T. J. Parker, and M. Lemmon, Dust devils vortices seen by the Mars Pathfinder Camera, *Geophys. Res. Lett.*, *26*, 2781–2785, 1999.

Murphy, J. R., and S. Nelli, Mars Pathfinder convective vortices: Frequency of occurrence, *Geophy. Res. Lett.*, *29*, 1–4, 2002.

Neubauer, F. M., Thermal convection in the Martian atmosphere, *J. Geophys. Res.*, *71*, 2419–2426, 1967.

Pollack, J. B., R. Haberle, R. Greeley, and J. Inversen, Estimates of the wind speeds required for particle motion on Mars, *Icarus*, *29*, 395–417, 1976.

Pollack, J. B., D. S. Colburn, R. Kahn, J. Hunter, W. Van Camp, C. E. Carlston, and M. R. Wolf, Properties of aerosols in the Martian atmosphere, as inferred from Viking Lander imaging data, *J. Geophys. Res.*, *82*, 4479–4496, 1977.

Pollack, J. B., D. S. Colburn, F. M. Flasar, R. Kahn, C. E. Carlston, and D. Pidek, Properties and effects of dust particles suspended in the Martian atmosphere, *J. Geophys. Res.*, *84*, 2929–2945, 1979.

Rennó, N. O., and A. P. Ingersol, Natural convection as a heat engine: A theory for CAPE, *J. Atmos. Sci.*, *53*, 572–585, 1996.

Rennó, N. O., M. L. Burkett, and M. P. Larkin, A simple thermodynamical theory for dust devils, *J. Atmos. Sci.*, *55*, 3244–3252, 1998.

Rennó, N. O., A. A. Nash, J. Lunine, and J. Murphy, Martian and Terrestrial dust devils: Test of a scaling theory using Pathfinder data, *J. Geophys. Res.*, *105*, 1859–1865, 2000.

Rover Team, Characterization of the Martian surface deposits by the Mars Pathfinder rover, Sojourner, *Science*, *278*, 1765, 1997.

Ryan, J. A., and R. D. Lucich, Possible dust devils, vortices on Mars, *J. Geophys. Res.*, *88*, 11,005–11,011, 1980.

Schofield, J. T., J. R. Barnes, D. Crisp, R. M. Haberle, S. Larsen, J. A. Magalhães, J. R. Murphy, A. Seiff, and G. Wilson, The Mars Pathfinder Atmospheric Structure Investigation/Meteorology (ASI/MET) experiment, *Science*, *278*, 1752–1758, 1997.

Seiff, A., and D. B. Kirk, Structure of the atmosphere of Mars in summer at mid-latitudes, *J. Geophys. Res.*, *82*, 4364–4377, 1977.

Smith, P. H., and M. Lemmon, Opacity of the Martian atmosphere measured by the imager for Mars Pathfinder, *J. Geophys.*, *104*, 1999.

Smith, P. H., et al., The imager for Mars Pathfinder experiment, *J. Geophys. Res.*, *102*, 4003–4026, 1997a.

Smith, P. H., et al., Results from the Mars Pathfinder Camera, *Science*, *278*, 1758–1764, 1997b.

Thomas, P., and P. Gierasch, Dust devils on Mars, *Science*, *230*, 175–177, 1985.

───────────────

F. Ferri, Center of Studies and Activities for Space (CISAS) "G. Colombo," University of Padova, I-35131 Padova, Italy. (francesca.ferri@unipd.it)

M. Lemmon, Texas A and M University, College Station, TX 77843, USA.

N. O. Rennó, Department of Atmospheric, Oceanic and Space Sciences, University of Michigan, Ann Arbor, MI 48109, USA.

P. H. Smith, Lunar and Planetary Laboratory, University of Arizona, Tucson, AZ 85721, USA.